Materials Science and Engineering B 210 (2016) 37–42

Contents lists available at ScienceDirect

Materials Science and Engineering B

journal homepage: www.elsevier.com/locate/mseb

The reactivity study of peptide A3-capped gold and silver nanoparticles with heavy metal ions

Hongyu Yang[a], Zhenghua Tang[a,b,*], Likai Wang[a], Weijia Zhou[a], Ligui Li[a], Yongqing Zhang[b], Shaowei Chen[a,c,*]

[a] New Energy Research Institute, School of Environment and Energy, South China University of Technology, Guangzhou Higher Education Mega Centre, Guangzhou 510006, China
[b] Guangdong Provincial Key Laboratory of Atmospheric Environment and Pollution Control, School of Environment and Energy, South China University of Technology, Guangzhou Higher Education Mega Centre, Guangzhou 510006, China
[c] Department of Chemistry and Biochemistry, University of California, 1156 High Street, Santa Cruz, CA 95064, United States

ARTICLE INFO

Article history:
Received 23 January 2016
Received in revised form 16 March 2016
Accepted 5 April 2016
Available online 4 May 2016

Keywords:
Peptide A3
Nanoparticle
Aggregation
Reaction
Heavy metal ions

ABSTRACT

Peptide A3-capped gold and silver nanoparticles were prepared by chemical reduction of metal salt precursors. The nanoparticles exhibited apparent but distinctly different color changes upon the addition of selected heavy metal ions. For gold nanoparticles, the solution color was found to change from red to blue in the presence of Hg^{2+} or As^{3+} ions, accompanied with broadening and a red-shift of the surface plasmon resonance peak. In contrast, silver nanoparticles showed an apparent color change from yellow to colorless only in the presence of Hg^{2+}, along with a blue-shift and diminishment of the surface plasmon resonance peak. The Hg^{2+} reaction concentration limit of silver nanoparticle was about 40 times lower than that of gold nanoparticle. Based on the dynamic light scattering, transmission electron microscopy and X-ray photoelectron spectroscopic results, the reaction mechanism has been proposed. Such a sensitive variation of the nanoparticle optical properties to selective ions might be exploited for ion detection for potential applications.

1. Introduction

Heavy metal pollution is one of the most serious environmental problems, as heavy metal ions are nonbiodegradable, highly toxic even at the trace level, and can accumulate in the food chain [1]. Heavy metal pollution undermines the public and human health, and has become a huge concern for global sustainability. Therefore, effective and sensitive monitoring of heavy metal ions has been of urgent importance. For instance, mercuric (Hg^{2+}) ions can easily penetrate biological membranes, and the uptake of Hg^{2+} ions can cause permanent damage to human brain, liver, the nerve system as well as other organs [2]. Arsenic (As^{3+}) ions are widely distributed in nature and even more toxic than Hg^{2+}. A trace amount of As^{3+} can exert detrimental effects on human health including carcinogenic diseases related to skin, lung, kidney, and others [3]. Therefore, a number of techniques, such as atomic emission spectroscopy, atomic absorption spectroscopy, and inductively coupled plasma-atomic emission spectroscopy, have been conventionally employed to detect and quantify heavy metal ions [4–6]. However, these methods typically involve expensive instrumentation, tedious sample preparation, sophisticated experimental procedures as well as specialized personnel. Colorimetric sensors based on nanostructured materials have been gaining increasing attention recently, thanks to their facile preparation, ease of operation, high sensitivity and extraordinary selectivity [7].

Among these, noble metal nanoparticles stabilized with DNA, peptides, proteins or other biomolecules have been found to exhibit remarkable propensity for the sensitive identification of heavy metal ions, mainly due to their characteristic surface plasmon resonance (SPR) properties [8–10]. In comparison with DNA or proteins, peptides possess distinct advantages such as low costs and rich diversity. As the nanoparticle physicochemical properties are associated with the binding interactions between the metal cores and peptide ligands, the peptide sequence can be modified to tune the size, shape and composition of the metal nanoparticles [11–14]. For instance, Wang and co-workers have recently developed a facile strategy to synthesize fluorescent gold nanoparticles with wavelength-tunable emissions using short peptides as templates,

* Corresponding authors at: New Energy Research Institute, School of Environment and Energy, South China University of Technology, Guangzhou Higher Education Mega Centre, Guangzhou 510006, China. Tel.: +86 2039381200.
E-mail addresses: zhht@scut.edu.cn (Z. Tang), shaowei@ucsc.edu (S. Chen).

http://dx.doi.org/10.1016/j.mseb.2016.04.001
0921-5107/

and used them for the sensitive detection of Hg^{2+} ions [14]. Despite a few successes have been achieved on peptide based nanoparticles as sensors for metal ions, yet, the reactivity between the peptide capped noble metal nanoparticles and metal ions have not been systematically studied. Specifically, if capped by the same sequence, how the reactivity differ from one type of metal nanoparticle (e.g. AuNPs) to another type of metal nanoparticle (e.g. AgNPs)? This is the primary motivation of the present study, where peptide A3-capped gold and silver nanoparticles were prepared and their reactivity were tested and compared for different metal ions.

Among the series of metal binding peptides, peptide A3, with a sequence of AYYSGAPPMPPF, is one of the few sequences that can stabilize both gold and silver nanoparticles with a desirable control of the size, shape and composition [15]. It contains amino acids that are capable of interacting with both gold and silver surfaces by hydrogen bonding or hydrophobic interactions [16–18]. For instance, Naik and co-workers prepared stable A3-capped silver and gold nanoparticles [15,19], and studied the reactions between metal ions and the nanoparticles [20], where Flg-A3 (sequence: DYKDDDDKAYSSGAPPMPPF) capped gold nanoparticles exhibited extraordinary colorimetric responses to several metal ions such as Co^{2+}, Hg^{2+}, Pb^{2+}, Pd^{2+}, and Pt^{2+}, while A3-AuNPs displayed almost negligible response to these metal ions. In other studies, Rosi and co-workers modified the N-terminus of the A3 sequence with hydrophobic dodecanoic acid for peptide assembly, and successfully prepared gold double helices [21] and hollow spheres [22,23].

Herein, we report the synthesis of peptide A3-capped gold and silver nanoparticles and their reactivity comparison for metal ions. Interestingly, among the 11 metal ions tested, peptide A3 capped gold nanoparticles (A3-AuNPs) exhibited a color change from red to blue upon the addition of Hg^{2+} or As^{3+} ions, accompanied with marked broadening and a red-shift of the surface plasmon peak, while peptide A3 capped silver nanoparticles (A3-AgNPs) showed a color change from yellow to colorless only in the presence of Hg^{2+}, with a blue-shift and diminishment of the surface plasmon peak, while no change in the presence of As^{3+} or other ions. For A3-AuNPs, the reaction was validated in the concentration range of 1–20 μM for Hg^{2+} and 10–50 μM for As^{3+}. For A3-AgNPs, the reaction was validated in the concentration range of 25 nM–20 μM for Hg^{2+}, with good linearity ($R^2 = 0.99$) and a concentration limit as low as 25 nM. The different colorimetric responses might be attributed to a variation of the mechanisms. Based on the results from transmission emission microscopy, dynamic light scattering, and X-ray photoelectron spectroscopy, two mechanisms have been proposed. For A3-AuNPs, Hg^{2+} or As^{3+} can adsorb on the metal cores and caused aggregation of the nanoparticles, where the well-defined morphology of individual nanoparticle were preserved. In contrast, for A3-AgNPs, the adsorption of Hg^{2+} onto the nanoparticle surface led to the formation of large amorphous bulky materials.

2. Materials and methods

2.1. Chemicals

Hydrogen tetrachloroauric acid ($HAuCl_4$) was purchased from Accela ChemBio Co., Ltd. while sodium borohydride ($NaBH_4$) and 4-(2-hydroxyerhyl) piperazine-1-ethanesulfonic acid (HEPES) were acquired from Aladdin Industrial Corporation (Shanghai, China). $ZnCl_2$, $FeCl_3$, $FeSO_4$, $CaCl_2$, $MnCl_2$, $MgCl_2$, $Pb(NO_3)_2$, $CoCl_2$, $Hg(NO_3)_2$ and $As_2(SO_4)_3$ were also purchased from Aladdin Industrial Corporation (Shanghai, China). Silver Nitrate ($AgNO_3$) was purchased from Sinopharm Chemical Reagents Co., Ltd. Peptide A3 (sequence AYSSGAPPMPPF, PURITY: >99%) was purchased from Top-Peptide (Shanghai, China), with purity confirmed by high performance liquid chromatographic (HPLC) separation and mass spectrometric (MS) analysis. All chemicals were used as received without further purification. Water was supplied with a Barnstead Nanopure Water System (18.3 MΩ cm).

2.2. Synthesis of Au and Ag nanoparticles

A3-capped nanoparticles were synthesized by adopting a protocol reported previously in the literature [12,19]. For the synthesis of A3-AuNPs, 0.5 mL of a peptide A3 aqueous solution (2.0 mM) and 0.6 mL of a HEPES buffer (1.00 mM, pH 7.2) were first mixed, into which was then added 3.869 mL of Nanopure water. The solution was stirred for 15 min, followed by the addition of 31 μL of a 0.096 M $HAuCl_4$ aqueous solution, corresponding to an Au:A3 molar feed ratio of 3:1. The solution was stirred for at least 15 min, where the solution color was found to gradually change from yellow to dark red, suggesting the formation of gold nanoparticles. The nanoparticle solution was under magnetic stirring for 15 min before being loaded into a semi-permeable membrane tube for dialysis in nanopure water, affording purified A3-AuNPs.

For the synthesis of A3-AgNPs, 500 μL peptide aqueous solution (2.0 mM) was added into 4.20 mL nanopure water, and then 0.1 mL of a 0.02 M $AgNO_3$ solution (corresponding to an Ag:A3 molar feed ratio of 2:1) was added. The resulting solution was stirred for 15 min, following by the addition of 0.2 mL freshly prepared $NaBH_4$ solution (0.01 M). The appearance of a dark yellow color signified the formation of silver nanoparticles. The nanoparticles were then also purified by dialysis in nanopure water.

2.3. Reactivity test with different metal ions

The A3-capped Au or Ag nanoparticles prepared above were then used for metal ion reaction. In a typical experiment, 0.4 mL of a 0.6 mM nanoparticle solution and 2.48 mL of nanopure water were added into a 4.0 mL quartz cuvette. A calculated amount of a metal ion solution (0.12 mL, 0.5 mM) was then injected into the cuvette by a syringe. The total volume of the solution was kept at 3.0 mL. The final concentrations of A3-AuNPs or A3-AgNPs and metal ions were 80 μM and 20 μM, respectively.

2.4. Characterizations

UV–vis absorption of the A3-AuNPs and A3-AgNPs was measured using a Shimadzu 2600/2700 UV–vis scanning spectrophotometer with a 1 cm quartz cuvette. Hydrodynamic radii of the nanoparticles were quantified by using a DynaPro Nanostar dynamic light scattering instrument (Wyatt Technology, USA). XPS analysis was conducted with an Escalab 250 photoelectron spectrometer (XPS, Thermo Fisher Scientific, USA). TEM measurements were recorded on a Tecnai G2-F20 microscope at an acceleration voltage of 100 kV. The TEM samples were prepared by dropcasting a nanoparticle dispersion directly onto a copper grid coated with a holy carbon film.

3. Results and discussions

3.1. Absorbance change of A3-AuNPs with different metal ions

Fig. 1 depicts the absorption spectra of A3-AuNPs in the absence and presence of 11 different metal ions. One can see that the as-produced A3-AuNPs (black curve) display an exponential decay profile, due to the Mie scattering of nanosized metal colloids [24–26], onto which is superimposed with a surface plasmon peak at 520 nm. Upon the addition of heavy metal ions, only a slight change of the peak intensity can be observed for most metal ions (e.g., Mg^{2+}, Ca^{2+}, Fe^{2+}, Fe^{3+}, Zn^{2+}, Pb^{2+}, and Cu^{2+}) whereas the peak position (solution color) remained virtually unchanged (figure

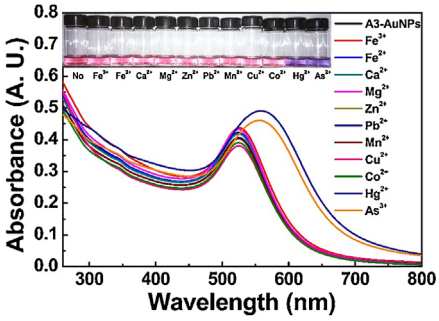

Fig. 1. UV–vis absorption spectra of A3-AuNPs upon the addition of various metal ions. The concentrations of A3-AuNPs and metal ions are 80 μM and 20 μM, respectively. Inset is the photographic images of A3-AuNPs before and after the addition of various metal ions.

inset), indicating no apparent interaction between the nanoparticles and metal ions. In sharp contrast, upon the addition of Hg^{2+} (blue curve) and As^{3+} (orange curve) ions, the surface plasmon peak can be found to be broadened and red-shift markedly, from 520 nm to 578 nm and 572 nm, respectively. Concurrently, the colors of these two solutions changed rapidly from red to purple/blue, indicating the size increase upon the addition of metal ions, as manifested in the figure inset. Consistent results were obtained in DLS measurements (Fig. 2), where the as-prepared A3-AuNPs were well dispersed with an average hydrodynamic radius (R_H) of 26.5 nm; however, upon the addition of Hg^{2+} or As^{3+}, R_H increased markedly to 261.6 nm and 142.5 nm, respectively, consistent with the formation of large nanoparticle aggregates.

3.2. DLS measurement of A3-AuNPs with Hg^{2+} or As^{3+}

According to the DLS measurements, the average radius of A3-AuNPs is about 26.5 nm (Fig. 2a). After adding Hg^{2+} and As^{3+} ions, the average size increased to 261.6 nm (Fig. 2b) and 142.5 nm (Fig. 2c). The Hg^{2+} and As^{3+} ion can absorb onto the metal core surface, which led to the nanoparticle aggregation and subsequent size increase. Consistent results were obtained in TEM measurements. Fig. S1 (a–c) depicts the TEM micrographs of the A3-AuNPs before and after the addition of Hg^{2+} or As^{3+} ions. It can be seen that the as-prepared A3-AuNPs were well separated and spherical in shape with an average diameter of 9.42 ± 1.58 nm (Fig. S1 (a and d)). However, after the addition of (b) Hg^{2+} or (c) As^{3+} ions, large aggregates can be easily seen, in good agreement with the DLS results. Yet, individual nanoparticle remained recognizable; and the average nanoparticle diameter was found to increase to 12.45 ± 2.30 nm (Fig. S1 (e)) and 11.47 ± 1.78 nm (Fig. S1 (f)), respectively. In contrast, in the presence of other ions in the series, no apparent aggregation of nanoparticles was observed (not shown).

3.3. XPS analysis of A3-AuNPs with Hg^{2+} or As^{3+}

Further structural insights were obtained in XPS measurements. From Fig. 3, it can be seen that for the as-produced A3-AuNPs, Au4f electrons exhibit two peaks at ($4f_{5/2}$) 86.1 eV and ($4f_{7/2}$) 82.4 eV, consistent with those of metallic Au(0) [27–30]. However, upon the addition of Hg^{2+} and As^{3+} ions, the binding energy of the Au4f electrons blue-shifted by ca. 0.4 eV to 86.5 and 82.8 eV, most likely due to ion adsorption and significant electron transfer from Au to the adsorbed ions. This suggests strong metallophillic interactions of gold nanoparticle cores with both Hg^{2+} and As^{3+} ions. Note that,

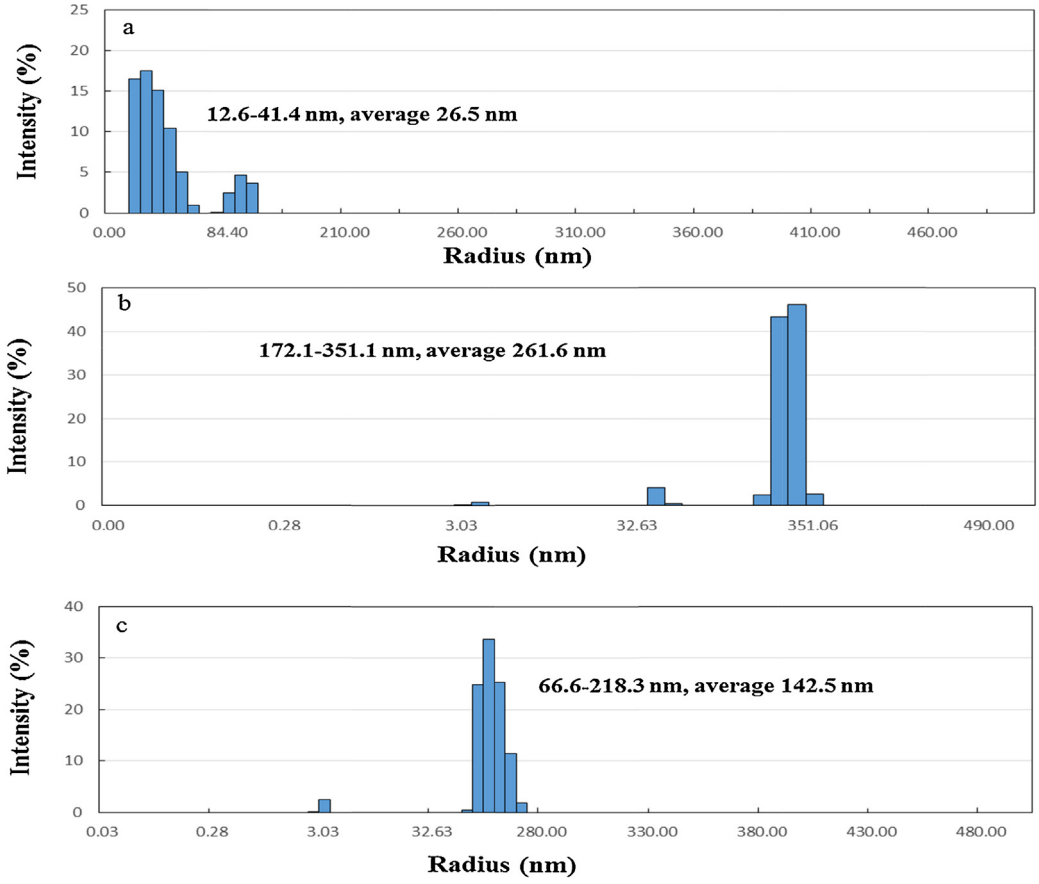

Fig. 2. DLS data of A3-AuNPs (a) before and after the addition of (b) Hg^{2+} and (c) As^{3+}. Experimental conditions are the same as those in Fig. 1.

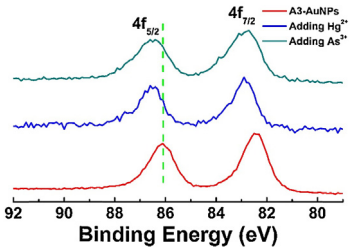

Fig. 3. XPS spectra of Au4f electrons of A3-AuNPs (red curve) before and after the addition of (blue curve) Hg^{2+} and (green curve) As^{3+} ions. For interpretation of the color information in this figure legend, the reader is referred to the web version of the article.)

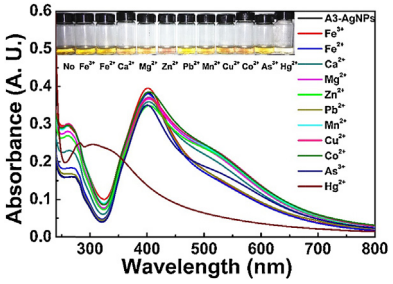

Fig. 5. UV–vis spectra of A3-AgNPs in the absence and presence of 11 types of metal ions. The concentrations of A3-AgNPs and metal ions are 80 μM and 20 μM, respectively. Inset depicts the corresponding photographs of the A3-AgNPs solutions with the addition of various metal ions.

unlike Hg^{2+} [31,32], reports of As^{3+} adsorption of on gold nanoparticles have been scarce, to the best of our knowledge. Such strong metallophillic interactions between the np core and Hg^{2+} or As^{3+} ions led to the aggregation of AuNPs, resulting in size increase subsequently. The aggregation did not destroy the well-defined morphology of the AuNPs, evidenced by the TEM results observed (Fig. S1).

3.4. Concentration dependent behavior of A3-AuNPs with Hg^{2+} or As^{3+}

To quantify the reaction concentration limit of A3-AuNPs for Hg^{2+} and As^{3+}, UV–vis absorption profiles of A3-AuNPs were collected with the addition of these two metal ions at different concentrations, as depicted in Fig. 4(a). It can be seen that upon the addition of 1 μM Hg^{2+} (top panel), the surface plasmon peak intensity enhanced slightly while the peak position remained unchanged at 520 nm. When the concentration was increased to 5 μM, the surface plasmon peak became broadened and shifted to a higher wavelength position (542 nm). At higher concentrations, a further red-shift of the peak can be seen. For instance, at the Hg^{2+} concentration of 20 μM, the peak position now reached 578 nm. Based on these measurements, the reaction limit concentration for Hg^{2+} ions was identified to be between 1 μM and 5 μM. Accordingly, the solution color changed from deep red to purple (inset to top panel). Similar phenomena can be seen for the reaction of A3-AuNPs with As^{3+} (bottom panel). With the addition of 10 μM As^{3+}, the surface plasmon peak position remained virtually unchanged at 520 nm while the intensity increased slightly. However, at 15 μM As^{3+}, the surface plasmon peak became broadened and shifted to a higher wavelength (539 nm). With the addition of an increasing amount of As^{3+}, the surface plasmon peak kept red-shifting until 40 μM where the peak position remained steady at 582 nm. It is interesting to notice that higher concentrations (e.g., 40 μM and 50 μM) did not shift the peak position any further. The solution color exhibited a similar color change as that observed with Hg^{2+} ions (Fig. 4(b)).

From these measurements, the reaction limit concentration for As^{3+} was estimated to be between 10 μM and 15 μM.

3.5. Absorbance change of A3-AgNPs with metal ions

The reactivity of A3-AgNPs was also examined with the same series of metal ions. Fig. 5 depicts the UV–vis absorption spectra of A3-AgNPs before and after the addition of various metal ions. The as-produced A3-AgNPs show a strong absorption peak at 400 nm, which is the surface plasmon resonance characteristic of silver nanoparticles [12]. Upon the addition of metal ions, apparent changes of the optical absorption were observed only in the presence of Hg^{2+} ions, where the surface plasmon peak diminished markedly, and virtually no change with other ions, even As^{3+}. Note that the reaction of A3-AgNPs with Hg^{2+} ions occurred very fast, evidenced by the formation of black precipitates at the bottom of the reaction vial in just a few minutes. This is likely due to the reaction between the silver nanoparticle cores and Hg^{2+} ions and the formation of zero-valence Hg or Ag/Hg amalgam [33].

3.6. DLS measurement of A3-AgNPs with Hg^{2+}

Consistent results were obtained in DLS measurements (Fig. 6). Before the addition of Hg^{2+}, the A3-AgNPs were well dispersed with an average R_H of 26.8 nm; and upon the addition of Hg^{2+}, R_H increased to 55.1 nm. TEM studies provide further insights to the structural evolution. Fig. S2 depicts the representative micrographs before and after the addition of Hg^{2+} ions. One can see that the as-produced A3-AgNPs were spherical in shape and well dispersed with an average core diameter of 9.83 ± 4.41 nm. After the addition of Hg^{2+} ions, large chunks (20–120 nm) of irregular shaped materials were formed, in good accord with the DLS results. It is worth noting that individual nanoparticles disappeared. This suggests the reaction between the Ag nanoparticles and Hg^{2+} ions. Such behaviors have been observed previously [34] where the adsorption of Hg^{2+} ions on mercaptosuccinic acid-protected silver nanoparticles

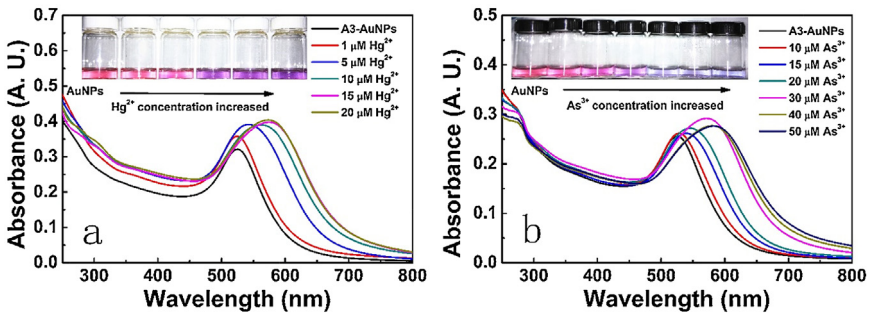

Fig. 4. UV–vis spectra of A3-AuNPs with the addition of (left) Hg^{2+} and (right) As^{3+} at different concentrations.

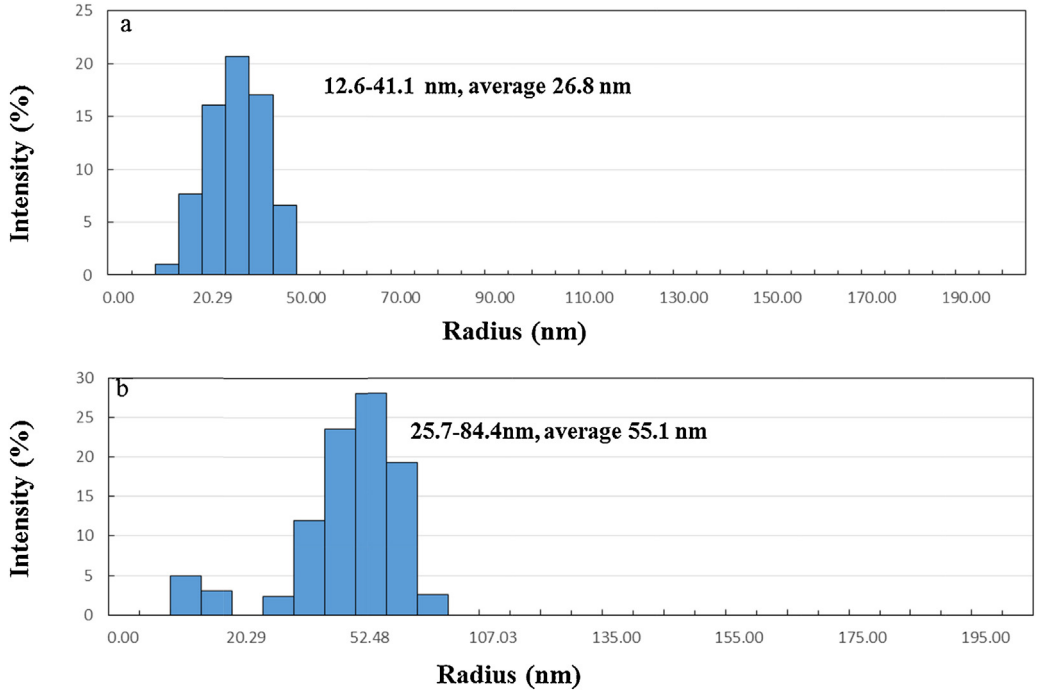

Fig. 6. DLS data of A3-AgNPs (a) before and (b) after the addition of Hg^{2+}. Experimental conditions are the same as those in Fig. 5.

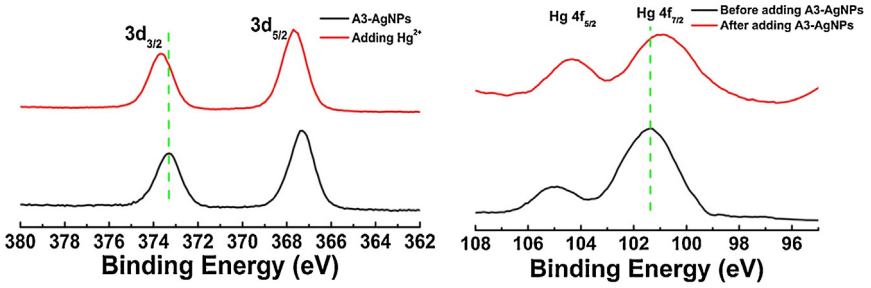

Fig. 7. XPS spectra of Ag3d electrons of A3-AgNPs in the absence and presence of Hg^{2+} (left) and Hg4f electrons before and after added into A3-AgNPs solution (right).

led to the reaction between the silver nanoparticle core and Hg^{2+} ions and the formation of large bulky materials.

3.7. XPS analysis of A3-AgNPs with Hg^{2+}

Subsequently, the XPS study of Ag 3d electrons of A3-AgNPs before and after adding Hg^{2+} and Hg4f electrons before and after added into A3-AgNPs solution (Fig. 7) was conducted. One can see that for the as-prepared A3-AgNPs, the binding energy of Ag $3d_{3/2}$ electrons was found at 373.3 eV, consistent with metallic Ag(0); yet, upon the addition of Hg^{2+} ions, the binding energy blue-shifted to 373.7 eV by 0.4 eV [30]. Meanwhile, the binding energy of Hg4f electrons decreased once Hg^{2+} ions were added into the A3-AgNPs solution, e.g. from 101.4 eV to 101 eV for Hg $4f_{7/2}$ electrons, indicating some Hg^{2+} ions were reduced into Hg^{+} or Hg(0). Again, this suggests substantial charge transfer from Ag to Hg^{2+} ions. Note that the mechanism is different from the AuNPs. As observed from TEM results, large bulk particles with amorphous shape were obtained, indicating a reaction instead of nanoparticle aggregation occurred. This is probably due to the reaction between the metal core and Hg^{2+} and the formation of Ag/Hg amalgam. Such a behavior is probably driven by the different formal potential between the Ag^{+}/Ag (+0.79 V) and Hg^{2+}/Hg (+0.85 V) couples.

3.8. Concentration dependent behavior of A3-AgNPs with Hg^{2+}

We then monitored the optical response of the A3-AgNPs with the addition of different concentrations of Hg^{2+} ions. From Fig. 8, it can be seen that upon the addition of 25 nM Hg^{2+}, whereas the solution color remained yellow (figure inset), the intensity of the surface plasmon peak dropped markedly. As increasing Hg^{2+} ion concentrations, the peak intensity decreased accordingly. For instance, at the Hg^{2+} concentration of 1 μM, the yellow color of the

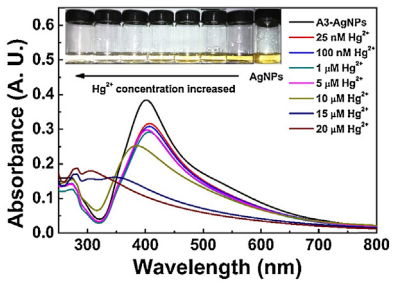

Fig. 8. UV–vis absorbance of A3-AgNPs reacting with Hg^{2+} of different concentrations. Higher concentration of Hg^{2+} resulted in the rapid color diminishing. Insert are the photographic images of A3-AgNPs and after adding Hg^{2+} with different concentrations.

nanoparticle solution began fading away, and totally vanished at 10 μM. In fact, the peak intensity exhibited a well-defined linear correlation with the concentration of Hg^{2+} ions ($R^2 = 0.99$), as shown in Figure S3.

4. Conclusions

In summary, we have systematically investigated the reactivity between peptide A3-capped gold and silver nanoparticles and metal ions. Among the 11 metal ions, A3-AuNPs exhibited marked optical responses to both Hg^{2+} and As^{3+} ions, as manifested by the red-shift of the A3-AuNPs surface plasmon resonance peak which was attributed to nanoparticle aggregation induced by Hg^{2+} or As^{3+}. A3-AgNPs exhibited much higher sensitivity to Hg^{2+} than A3-AuNPs, but no response to As^{3+}. It was postulated that the observed blue-shift and diminishment of the A3-AgNPs surface plasmon peak was due to the reaction between the nanoparticle metal core and Ag^{+} and formation of large bulky materials. Consistent results were obtained in TEM, DLS and XPS measurements. The Hg^{2+} reaction concentration limit of A3-AgNPs can be as low as 25 nM, which is about 40 times lower than that of A3-AuNPs. Such a sensitive variation of the nanoparticle optical properties to selective ions might be exploited for ion detection for potential applications in future.

Acknowledgements

This work was partially supported by the National Recruitment of Global Experts and the National Natural Science Foundation of China (NSFC 21528301). T.Z.H. acknowledges financial support from the Fundamental Research Funds for Central Universities (SCUT grant No. 2015ZM012 and 2015PT026), Project of Public Interest Research and Capacity Building of Guangdong Province (2015A010105009) and Guangdong Natural Science Funds for Distinguished Young Scholars (No. 2015A030306006).

Appendix A. Supplementary data

Supplementary data associated with this article can be found, in the online version, at http://dx.doi.org/10.1016/j.mseb.2016.04.001.

References

[1] G. Aragay, J. Pons, A. Merkoçi, Chem. Rev. 111 (2011) 3433.
[2] E.M. Nolan, S.J. Lippard, Chem. Rev. 108 (2008) 3443.
[3] S. Shen, X.-F. Li, W.R. Cullen, M. Weinfeld, X.C. Le, Chem. Rev. 113 (2013) 7769.
[4] B.N. Kumar, D.K.V. Ramana, Y. Harinath, K. Seshaiah, M.C. Wang, J. Agric. Food Chem. 59 (2011) 11352.
[5] A. Imyim, P. Daorattanachai, F. Unob, Anal. Lett. 46 (2013) 2101.
[6] P.C. Zheng, B. Zhang, J.M. Wang, X.M. Wang, H.D. Liu, R. Yang, Spectrosc. Spect. Anal. 35 (2015) 2012.
[7] M. Li, H. Gou, I. Al-Ogaidi, N. Wu, ACS Sustainable Chem. Eng. 1 (2013) 713.
[8] K.M. Mayer, J.H. Hafner, Chem. Rev. 111 (2011) 3828.
[9] J. Du, L. Jiang, Q. Shao, X. Liu, R.S. Marks, J. Ma, X. Chen, Small 9 (2013) 1467.
[10] M.R. Knecht, M. Sethi, Anal. Bioanal. Chem. 394 (2009) 33.
[11] Z. Tang, J.P. Palafox-Hernandez, W.-C. Law, Z.E. Hughes, M.T. Swihart, P.N. Prasad, M.R. Knecht, T.R. Walsh, ACS Nano 7 (2013) 9632.
[12] J.P. Palafox-Hernandez, Z. Tang, Z.E. Hughes, Y. Li, M.T. Swihart, P.N. Prasad, T.R. Walsh, M.R. Knecht, Chem. Mater. 26 (2014) 4960.
[13] B.D. Briggs, M.R. Knecht, J. Phys. Chem. Lett. 3 (2012) 405.
[14] J.-J. Feng, H. Huang, D.-L. Zhou, L.-Y. Cai, Q.-Q. Tu, A.-J. Wang, J. Mater. Chem. C 1 (2013) 4720.
[15] R.R. Naik, S.J. Stringer, G. Agarwal, S.E. Jones, M.O. Stone, Nat. Mater. 1 (2002) 169.
[16] J.M. Slocik, D.W. Wright, Biomacromol 4 (2003) 1135.
[17] R. Lévy, N.T.K. Thanh, R.C. Doty, I. Hussain, R.J. Nichols, D.J. Schiffrin, M. Brust, D.G. Fernig, J. Am. Chem. Soc. 126 (2004) 10076.
[18] S. Brown, Nano Lett. 1 (2001) 391.
[19] J.M. Slocik, M.O. Stone, R.R. Naik, Small 1 (2005) 1048.
[20] J.M. Slocik, J.S. Zabinski, D.M. Phillips, R.R. Naik, Small 4 (2008) 548.
[21] C.-L. Chen, P. Zhang, N.L. Rosi, J. Am. Chem. Soc. 130 (2008) 13555.
[22] C.-L. Chen, N.L. Rosi, J. Am. Chem. Soc. 132 (2010) 6902.
[23] C. Song, G. Zhao, P. Zhang, N.L. Rosi, J. Am. Chem. Soc. 132 (2010) 14033.
[24] M.M. Alvarez, J.T. Khoury, T.G. Schaaff, M.N. Shafigullin, I. Vezmar, R.L. Whetten, J. Phys. Chem. B 101 (1997) 3706.
[25] S.L. Logunov, T.S. Ahmadi, M.A. ElSayed, J.T. Khoury, R.L. Whetten, J. Phys. Chem. B 101 (1997) 3713.
[26] J.S. Melinger, V.D. Kleiman, D. McMorrow, F. Gröhn, B.J. Bauer, E. Amis, J. Phys. Chem. A 107 (2003) 3424.
[27] M.-C. Bourg, A. Badia, R.B. Lennox, J. Phys. Chem. B 104 (2000) 6562.
[28] P. Zhang, J. Phys. Chem. C 118 (2014) 25291.
[29] Z. Tang, D.A. Robinson, N. Bokossa, B. Xu, S. Wang, G. Wang, J. Am. Chem. Soc. 133 (2011) 16037.
[30] K. Heister, M. Zharnikov, M. Grunze, L.S.O. Johansson, J. Phys. Chem. B 105 (2001) 4058.
[31] J. Xie, Y. Zheng, J.Y. Ying, Chem. Commun. 46 (2010) 961.
[32] L. Shang, L. Yang, F. Stockmar, R. Popescu, V. Trouillet, M. Bruns, D. Gerthsen, G.U. Nienhaus, Nanoscale 4 (2012) 4155.
[33] F.-L. Mi, S.-J. Wu, W.-Q. Zhong, C.-Y. Huang, Phys. Chem. Chem. Phys. 17 (2015) 21243.
[34] E. Sumesh, M.S. Bootharaju, T. Anshup, Pradeep, J. Hazard. Mater. 189 (2011) 450.